arXiv:1003.1614v2 [cond-mat.mes-hall] 26 May 2010

Unique Electron Spin Relaxation Induced by Confined Phonons in Nanowire-Based Quantum Dots

Y. Yin and M. W. Wu[*]

Hefei National Laboratory for Physical Sciences at Microscale and Department of Physics,
University of Science and Technology of China, Hefei, Anhui, 230026, China

(Dated: May 27, 2010)

Electron spin relaxation in nanowire-based quantum dots induced by confined phonons is investigated theoretically. Due to the one-dimensional nature of the confined phonons, the van Hove singularities of the confined phonons and the zero of the form factor of the electron-phonon coupling can lead to unique features of the spin relaxation rate. Extremely strong spin relaxation can be obtained at the van Hove singularity. Meanwhile the spin relaxation rate can also be greatly suppressed at the zero of the form factor. This unique feature indicates the flexibility of nanowire-based quantum dots in the manipulation of spin states. It also offers a way to probe the property of the confined phonons.

PACS numbers: 72.25.Rb, 63.22.-m, 73.21.La, 63.20.kd

Electron spin relaxation in semiconductor quantum dots (QDs) has been an important problem due to the proposed application of spin states in QDs as qubits for quantum computation.[1,2] QDs with the spin-orbit coupling are of particular interest since they enable efficient manipulations of spin with electric field.[3–5] Typical III-V semiconductor QDs are either self-assembled ones or fabricated by confining electrons in quantum wells by electrodes, where bulk phonons in substrates play an important role.[6–10] For these QDs, the acoustic bulk phonons in conjunction with the spin-orbit coupling serve as the main source for spin relaxation in low-temperature regime.[7] Recently, QDs based on III-V compound semiconductor nanowires were fabricated.[11–13] The nanowires are perpendicular to the substrate, making the bulk phonons in substrate less important than the confined phonons in nanowires.[14,15] The regular structure of the nanowires results in the quasi-one-dimensional confined phonons, which lead to novel properties in optical absorption and transport for the nanowire-based QDs.[16,17] In this Report, we show that the confined phonons lead to unique behaviors of the spin relaxation in elongate QDs embedded in nanowires.

We focus here on a single-electron elongate QD embedded in InAs [001] cylindrical nanowire with radius R in the presence of an external magnetic field B along the wire. We model the QD by an anisotropic harmonic potential $V_c(r,z)=\frac{1}{2}m^*\omega_0^2r^2+\frac{1}{2}m^*\omega_z^2z^2$ with z-axis along the wire and $\omega_0 \gg \omega_z$ so that only the lowest electron subband in the radial direction is needed.[18] m^* is the effective mass of the electron. Thus the size of the QD is decided by the diameter $d_0=\sqrt{\hbar\pi/m^*\omega_0}$ in radial direction and the length $d_z=\sqrt{\hbar\pi/m^*\omega_z}$ in axial direction. The spin-orbit coupling in the QD is described by the Rashba term $H_{\rm SO}=\frac{\gamma}{\hbar}\sigma_y p_z$, where $\gamma = 3.0\times 10^{-11}$ eV·m is Rashba coupling constant[19] and σ_y is the Pauli matrix.

Due to the well separated energy levels of the QD, the spin relaxation rate (SRR) can be described by the scattering rate between the two lowest eigenstates $|i\rangle$ and $|f\rangle$ with opposite spin orientations, which can be calculated by the Fermi golden rule.[8–10,20,21] Treating $|i\rangle$ and $|f\rangle$ as the initial and final states, at zero temperature the SRR can be written as

$$\Gamma_{fi}=\sum_{m\nu}\frac{|M_\nu(\boldsymbol{q}_m)G_{fi}(\nu,\boldsymbol{q}_m)|^2}{|\partial_{\boldsymbol{q}_m}(\hbar\omega_\nu(\boldsymbol{q}_m))|}\theta(\Delta\varepsilon_{fi})\Bigg|_{\hbar\omega_\nu(\boldsymbol{q}_m)=\Delta\varepsilon_{fi}}, \tag{1}$$

where $\Delta\varepsilon_{fi}=\varepsilon_i-\varepsilon_f$ is the energy splitting between the two states and $\theta(\varepsilon)$ is the step function. $M_\nu(\boldsymbol{q})G_{fi}(\nu,\boldsymbol{q})$ describes the matrix element of the electron-phonon coupling with $G_{fi}(\nu,\boldsymbol{q})$ being the form factor, which depends not only on the electron wave function but also on the phonon eigenmode for confined phonons. $\hbar\omega_\nu(\boldsymbol{q})$ is the phonon spectrum. The summation m is performed over the surface of the constant energy.

Poles in Eq. (1) correspond to the van Hove singularities. For bulk phonons, since the constant-energy surface is continuous, the SRR does not diverge after the integration. However, for confined phonons, the constant-energy surface reduces to discrete points, so the SRR can be divergent if the energy splitting $\Delta\varepsilon$ matches the van Hove singularities. Similarly, the SRR can also be suppressed by the zero of the form factor $G_{fi}(\nu,\boldsymbol{q})$. These features can be served as the fingerprints of the confined phonons. We will show that these unique features of the SRR can be realized in typical nanowire-based QDs.[11–13] We mainly focus on the electron-phonon interaction due to the deformation potential coupling, since it is dominant for small semiconductor nanostructures.[22]

We calculate the confined phonons with isotropic elastic continuum model which is widely used in the study of nanowires, carbon nanotubes and nanoparticles.[22–27] The nanowire is modeled as an infinite cylinder with the stress vanishing at the surface of the wire. Since we only consider the lowest subband of the electron in the radial direction, due to the conservation of the angular momentum, only phonon modes with zero angular momentum can couple to electrons by the deformation-potential coupling.[28] These modes are usually referred as the dilatation modes.[23,26,27]

We set the nanowire radius $R = 15$ nm which is a typical radius for the nanowires.[15] The other relevant parameters are the longitude and transverse sound velocities which are chosen to be $v_L = 3830$ m/s and $v_T = 2640$ m/s along the [001] direction.[29] The eigenmodes and spectrum $\hbar\omega_\nu(q)$ of the confined phonons are calculated following Refs. 30,31. The calculated spectra of the first six dilatation modes are plotted in Fig. 1(a) and the corresponding phonon density of the states (DOS) is shown in Fig. 1(b). The peaks in the DOS indicate the van Hove singularities which correspond to the minima of each phonon subband. It should be noted that there are two types of minima: minimum with $q = 0$ and $q \neq 0$. Modes 3, 5 and 6 correspond to the first type. For modes 2 and 4, in addition to the first type, there are minima with $q \neq 0$ ($q = 0.063$ nm^{-1} for mode 2 and 0.081 nm^{-1} for mode 4).

The lowest two eigenstates $|i\rangle$ and $|f\rangle$ can be calculated by treating the spin-orbit coupling as perturbation. Since only the lowest electron subband is considered, the radial component of the electron wave function is described by the cylindrical Gaussian function with width d_0. So the unperturbed state $|n_z\sigma\rangle$ can be characterized by the quantum number of the harmonic confinement along axial direction n_z and electron spin index σ. Up to the first-order perturbation, one has $|i\rangle = |0\uparrow\rangle + \mathcal{B}_-|1\downarrow\rangle$ and $|f\rangle = |0\downarrow\rangle + \mathcal{B}_+|1\uparrow\rangle$, where $\mathcal{B}_\pm = -\frac{\sqrt{2\pi}\gamma}{4d_z}/(g\mu_B B \pm \hbar\omega_z)$ with g and μ_B being the g factor of electron and Bohr magneton, respectively.[10] Note that for the QD considered here, the energy splitting induced by the spin-orbit coupling is much smaller than the Zeeman energy so it is adequate to have $\Delta\varepsilon = |g\mu_B B|$.

Given the two eigenstates and the phonon eigenmodes, the matrix element of the deformation-potential coupling $M_\nu(q)G_{fi}(\nu, q)$ can be calculated[28] with q being the axial phonon wave vector. The form factor is expressed as $G_{fi}(\nu, q) = I_z^d(q)I_{xy}^d(\nu, q)$ with $I_z^d(q)$ and $I_{xy}^d(\nu, q)$ being the axial and radial components. The axial component has the form $I_z^d(q) = d_z q e^{-(qd_z)^2/4\pi}$, which does not depend on the phonon mode index ν. The radial component can be written as

$$I_{xy}^d(\nu, q) = \chi_\nu^{(0)}(q)(k_L/d_0)^2 e^{A_L(\nu,q)}, \qquad (2)$$

with $k_{L,T} = \hbar\omega_\nu(q)/(\hbar v_{L,T})$ and $A_{L,T}(\nu, q) = (q^2 - k_{L,T}^2)d_0^2/(4\pi)$. $\chi_\nu^{(0)}(q)$ is the coefficient in the expression for the confined phonon eigenmode which are calculated numerically following Refs. 30,31. The corresponding coefficient $M_\nu(q)$ can be expressed as $M_\nu(q) = |\mathcal{B}_- + \mathcal{B}_+|^2\mathcal{C}^d/\Delta\varepsilon$. $\mathcal{C}^d = \hbar^3\Xi^2/(16Dv_L)$ is a constant where the deformation-coupling strength $\Xi = 5.8$ eV and density $D = 5900$ kg/m^3.[29] Given the matrix element $M_\nu(q)G_{fi}(\nu, q)$ and the phonon spectrum $\hbar\omega_\nu(q)$, the SRR can be calculated by Eq. (1). In the calculation, we set the size of the QD to be $d_z = 50$ nm and $d_0 = 12$ nm. $g = -14.7$.[29]

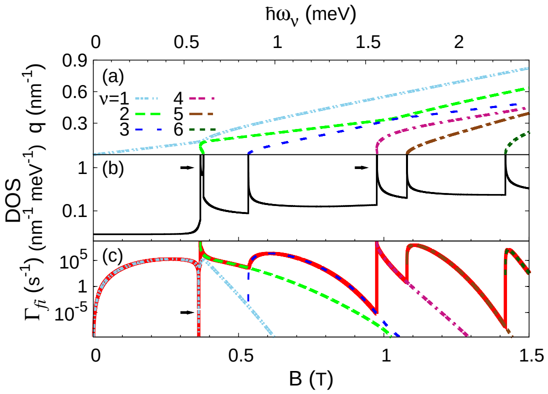

FIG. 1: (Color online) SRR as a function of external magnetic field B with QD diameter $d_0 = 12$ nm (shown in (c)). The corresponding phonon energy $\hbar\omega_\nu$ is given in the upper scale. (a) and (b) show the energy spectrum and DOS for dilatation phonon modes respectively. The red solid curve in (c) represents the total SRR. The contributions of each dilatation mode are plotted in (c) with different colors and line shapes. Curves with the same color and line shape in (a) and (c) correspond to the same phonon mode. The arrow in (c) indicates the dip induced by the zero of the form factor. The peaks in (b) indicated by the arrows correspond to the $q \neq 0$ van Hove singularities. The peak at $B = 0.975$ T in fact contains two peaks too close to see due to the scale.

The calculated SRR as a function of external magnetic field B is plotted in Fig. 1(c). Since the SRR is the summation of the contributions from each phonon mode, we plot them in the same figure with different colors/line shapes for comparison. It can be seen that the SRR as a function of B can be separated into several regions. In each region, only one phonon mode dominates. Thus the properties of individual phonon modes are crucial to the SRR. This makes the SRR very sensitive to the magnetic field B. Sharp peaks can be found in Fig. 1(c) at $B = 0.368$ T and $B = 0.975$ T, whereas a dip exists at the position indicated by the arrow.

Let us first concentrate on the sharp peaks in the SRR. Comparing to the DOS in Fig. 1(b), one can see that these peaks correspond to the van Hove singularities with $q \neq 0$. The SRR diverges at these singularities. For the van Hove singularities with $q = 0$, there is no divergence as the form factor tends to 0 at $q = 0$. Only broad peaks exist. To show this, we plot the form factor $G_{fi}(\nu, q)$ in Fig. 2. Similar behavior also exists in phonon satellites in the excitonic absorption.[16] Note that this behavior is different from the disk-shaped QDs embedded in the nanowires,[32] where the SRR diverges for singularities at $q = 0$. It is noted that the divergence of the SRR at the van Hove singularities originates from the approach of the Fermi golden rule Eq. (1), where the Markovian approximation is implied. However, the divergence of the SRR means the memory effect should not be neglected and one should apply the non-Markovian approach[33] to calculate

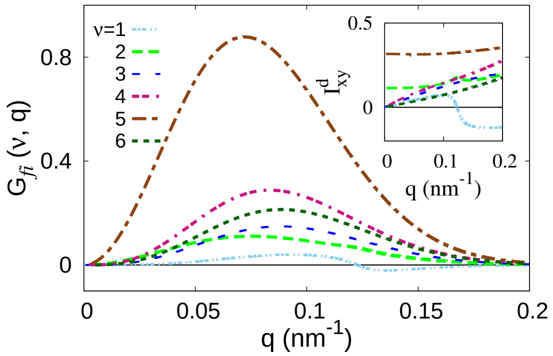

FIG. 2: (Color online) Form factor $G_{fi}(\nu, q)$ for the first six dilatation modes versus wave vector q. Inset is for the radial component $I^d_{xy}(\nu, q)$. Curve with the same color and line shape as that in Fig. 1 corresponds to the same dilatation mode.

the SRR around these singularities. This will remove the divergence. Moreover, other mechanisms, such as the phonon-phonon scattering, disorder, etc. can also remove the divergence by broadening. However, the peaks should still survive.

Now we turn to the dip in the SRR indicated by the arrow in Fig. 1(c). The dip results from the zero of the radial component $I^d_{xy}(\nu, q)$ of the form factor.[34] From Fig. 2, one can see that for phonon mode 1, $I^d_{xy}(\nu, q)$ has a zero point for $q \neq 0$. As a consequence, the deformation potential coupling of this mode vanishes at this point, making the SRR drop to zero rapidly. It is further noted that according to Eq. (2), the zero point of $I^d_{xy}(\nu, q)$ is just the zero of $\chi^{(0)}_\nu(q)$. So the dip in the SRR offers a way to probe the confined phonons.

In conclusion, we have calculated the SRR induced by confined acoustic phonons in elongate QDs embedded in InAs [001] nanowires. The SRR is dominated by individual confined phonon mode at different magnetic field region, which results in a highly nonmonotonic magnetic field dependence. Due to the one-dimensional nature of the confined phonons, the SRR limited by the spin-orbit coupling combined with the electron-phonon scattering can be divergent at the van Hove singularities of the phonons, provided the form factor does not go to zero at these singularities. Moreover, the zero of the form factor strongly suppresses the SRR, causing dips in the magnetic field dependence of the SRR. These features can be served as the fingerprints of the confined phonons. It is also seen from our calculation that the nanowire-based QDs can enable more flexible manipulations of spin states.

This work was supported by the Natural Science Foundation of China under Grant No. 10725417, the National Basic Research Program of China under Grant No. 2006CB922005 and the Knowledge Innovation Project of Chinese Academy of Sciences. One of the authors (MWW) would like to thank Guido Burkard for valuable discussions.

---

[*] Author to whom correspondence should be addressed; Electronic address: mwwu@ustc.edu.cn.

[1] D. Loss and D. P. DiVincenzo, Phys. Rev. A **57**, 120 (1998).

[2] R. Hanson, L. P. Kouwenhoven, J. R. Petta, S. Tarucha, and L. M. K. Vandersypen, Rev. Mod. Phys. **79**, 1217 (2007).

[3] E. I. Rashba and Al. L. Efros, Phys. Rev. Lett. **91**, 126405 (2003).

[4] Y. Kato, R. C. Myers, A. C. Gossard, and D. D. Awschalom, Nature (London) **427**, 50 (2004).

[5] V. N. Golovach, M. Borhani, and D. Loss, Phys. Rev. B **74**, 165319 (2006).

[6] V. N. Golovach, A. Khaetskii, and D. Loss, Phys. Rev. Lett. **93**, 016601 (2004).

[7] J. H. Jiang, Y. Y. Wang, and M. W. Wu, Phys. Rev. B **77**, 035323 (2008).

[8] A. V. Khaetskii and Y. V. Nazarov, Phys. Rev. B **61**, 12639 (2000); **64**, 125316 (2001).

[9] L. M. Woods, T. L. Reinecke, and Y. Lyanda-Geller, Phys. Rev. B **66**, 161318 (2002).

[10] J. L. Cheng, M. W. Wu, and C. Lü, Phys. Rev. B **69**, 115318 (2004).

[11] M. T. Björk, B. J. Ohlsson, T. Sass, A. I. Persson, C. Thelander, M. H. Magnusson, K. Deppert, L. R. Wallenberg, and L. Samuelson, Appl. Phys. Lett. **80**, 1058 (2002).

[12] M. T. Björk, C. Thelander, A. E. Hansen, L. E. Jensen, M. W. Larsson, L. R. Wallenberg, and L. Samuelson, Nano Lett. **4**, 1621 (2004).

[13] H. A. Nilsson, C. Thelander, L. E. Fröberg, J. B. Wagner, and L. Samuelson, Appl. Phys. Lett. **89**, 163101 (2006).

[14] B. J. Ohlsson, M. T. Björk, M. H. Magnusson, K. Deppert, L. Samuelson, and L. R. Wallenberg, Appl. Phys. Lett. **79**, 3335 (2001).

[15] H. Shtrikman, R. Popovitz-Biro, A. Kretinin, and M. Heiblum, Nano Lett. **9**, 215 (2009).

[16] G. Lindwall, A. Wacker, C. Weber, and A. Knorr, Phys. Rev. Lett. **99**, 087401 (2007).

[17] C. Weber, A. Fuhrer, C. Fasth, G. Lindwall, L. Samuelson, and A. Wacker, Phys. Rev. Lett. **104**, 036801 (2010).

[18] Strictly speaking, one has to use an axial asymmetric potential to describe the quantum dot in the nanowire, e.g., the center of the quantum dot is slightly displaced from the center of the nanowire, which induces the Rashba SOC. But one can prove that, up to the first order, the contribution of the displacement to the spin relaxation vanishes. So it is adequate to use the axial symmetric model in the calculation.

[19] D. Grundler, Phys. Rev. Lett. **84**, 6074 (2000).

[20] C. F. Destefani and Sergio E. Ulloa, Phys. Rev. B **72**, 115326 (2005).

[21] V. N. Golovach, A. Khaetskii, and D. Loss, Phys. Rev. B

77, 045328 (2008).

[22] T. Takagahara, Phys. Rev. Lett. **71**, 3577 (1993).

[23] A. N. Cleland, *Foundation of Nanomechanics* (Springer-Verlag, Berlin, 2003).

[24] H. Suzuura and T. Ando, Phys. Rev. B **65**, 235412 (2002).

[25] P. Chassaing, F. Demangeot, N. Combe, L. Saint-Macary, M. L. Kahn, and B. Chaudret, Phys. Rev. B **79**, 155314 (2009).

[26] S. Yu, K. W. Kim, M. A. Stroscio, and G. J. Iafrate, Phys. Rev. B **51**, 4695 (1995).

[27] S. M. Komirenko, K. W. Kim, M. A. Stroscio, and V. A. Kochelap, Phys. Rev. B **58**, 16360 (1998).

[28] N. Nishiguchi, Phys. Rev. B **54**, 1494 (1996).

[29] *Semiconductors Landolt-Börnstein*, edited by O. Madelung, Vol. 17a, (Springer-Verlag, Berlin, 1987).

[30] B. A. Auld, *Acoustic Fields and Waves in Solids* (Wiley, New York, 1973).

[31] M. A. Stroscio, K. W. Kim, S. Yu, and A. Ballato, J. Appl. Phys **76**, 4670 (1994).

[32] M. Trif, V. N. Golovach, and D. Loss, Phys. Rev. B **77**, 045434 (2008).

[33] P. Zhang and M. W. Wu, Phys. Rev. B **76**, 193312 (2007).

[34] Note that the axial component can also have zeros for hard-wall confinement in axial direction [see, D. V. Bulaev, B. Trauzettel, and D. Loss, Phys. Rev. B **77**, 235301 (2008)].